Dissociation Equilibrium of Human Recombinant Interferon γ[†]

Raina Boteva,*[,‡] Theodora Zlateva,[§] Victoria Dorovska-Taran,[||,⊥] Antonie J. W. G. Visser,[||] Roumen Tsanev,[‡] and Benedetto Salvato[§]

Institute of Molecular Biology and Institute of Organic Chemistry, Bulgarian Academy of Sciences, Sofia 1113, Bulgaria, CNR Centre of Metalloproteins, Department of Biology, University of Padua, 35121 Padua, Italy, and Department of Biochemistry, Agricultural University, Dreijenlaan 3, NL-6703 HA Wageningen, The Netherlands

Received November 21, 1995; Revised Manuscript Received June 27, 1996[⊗]

ABSTRACT: The biologically active form of interferon γ is a dimer composed of two noncovalently bound identical polypeptide chains of 17 kDa each. In this study, it was found that dissociation of the dimer into monomers significantly reduced the fluorescence quantum yield and the efficiency of the intermolecular Tyr to Trp radiationless energy transfer. The same process caused significant changes in the fluorescence decay and in the fluorescence anisotropy decay. The kinetic and thermodynamic parameters of the dimer−monomer equilibrium were determined by fluorescence measurements at different temperatures and by a theoretical mathematical model. Dissociation of the dimers into monomers was an endothermic process and was favored by concentrations of the protein lower than 1 μM and by increasing the temperature. It was accompanied by formation of aggregates, a slow and partially reversible process leading to inactivation of the interferon. It is suggested that certain monomeric conformers are competent for aggregation.

Interferon γ (IFN-γ)[1] is a cytokine produced in minute quantities by some activated T lymphocytes. Due to its various activities—antiviral, antiproliferative, immunoregulatory, and modulation of gene expression—this protein is used for the treatment of different diseases. Unfortunately, storage of unfrozen highly purified IFN-γ preparations even at low temperature and in the presence of stabilizing agents is accompanied by a gradual decrease of their antiviral activity (Pestka et al., 1987). Possible reasons for this spontaneous inactivation could be either slow irreversible changes in the active conformation of the molecule and/or processes of aggregation.

The X-ray crystal structures of recombinant human and rabbit IFN-γ have shown that they are α helical proteins containing six helices and no β sheet structure. Their active form is a dimer composed of two identical polypeptide chains, tightly associated by numerous interhelical interactions (Ealick et al., 1992; Samudzi et al., 1991). Sedimentation studies on human IFN-γ equilibria have registered dimers and oligomers but no monomers (Yphantis & Arakawa, 1987). Refolding of the protein denatured by urea, acid, or guanidine hydrochloride was found to yield two different forms: dimeric (active) and aggregated with a 4−8-fold-reduced activity (Arakawa et al., 1985; Arakawa & Hsu, 1987). Aggregation appears to be a complex process, probably involving various conformational intermediates and different phases. It is initiated during a lag phase which could last from a few minutes up to many days depending on the temperature (Mulkerrin & Wetzel, 1989). The dimers and aggregates have similar secondary but different tertiary structures in the local microenvironment of the aromatic amino acid residues as shown by UV circular dichroic spectra (Hsu & Arakawa, 1985).

There is no doubt that the stability of IFN-γ dimers should play a central role in maintaining the biological activity of the protein. However, extensive physicochemical studies on the dissociation of the dimer are lacking to date. In the present paper, we have studied and characterized the dimer−monomer equilibrium of recombinant human IFN-γ by both static and dynamic fluorescence measurements. We have followed the effects of temperature, protein concentration, and time on the intrinsic protein fluorescence and have registered conformational changes which parallel the formation of different forms: dimers, monomers, and aggregates.

MATERIALS AND METHODS

Human recombinant interferon γ (hrIFN-γ) was a product of Pharmagen Ltd., Sofia. It does not contain the leader sequence Cys-Tyr-Cys or the N-terminal methionine and has a purity of 99.5%, as judged by HPLC and gel electrophoresis. Its specific activity is about 5×10^7 IU/mg as determined by using the 50% protection value of interferon dilution against the cytopathic effect of VSV on WISH cells (Rubinstein et al., 1981).

Protein concentration was determined by the procedure of Lowry (1951) and by using a molar extinction coefficient at 280 nm of 1.1×10^4 M^{-1} cm^{-1} calculated on the basis of the aromatic amino acid content (Beaven & Holiday, 1952).

Fluorescence was measured with a Perkin-Elmer model MPF-43 spectrofluorometer equipped with a thermostatically controlled cuvette holder. Excitation was at either 270 or 295 nm. The relative Trp quantum yield was calculated by comparing the integrated emission spectrum of the protein

[†] This work was supported by a grant from the Bulgarian National Committee for Science, partially supported by a grant from Padua University to T.Z., and supported by a fellowship of the Wageningen Agricultural University to V.D.-T.

* Corresponding author. Telephone: (359-2) 713-2641. Fax: (359-2) 72 35 07.

[‡] Institute of Molecular Biology, Bulgarian Academy of Sciences.

[§] University of Padua.

[||] Agricultural University.

[⊥] Institute of Organic Chemistry, Bulgarian Academy of Sciences.

[⊗] Abstract published in *Advance ACS Abstracts,* October 1, 1996.

[1] Abbreviations: hrIFN-γ, human recombinant interferon γ; HPLC, high-pressure liquid chromatography; MEM, maximal entropy method; PAGE, polyacrylamide gel electrophoresis; N-Ac-Trp-NH_2, *N*-acetyl-L-tryptophanamide; VSV, vesicular stomatitis virus.

S0006-2960(95)02759-0 CCC: $12.00

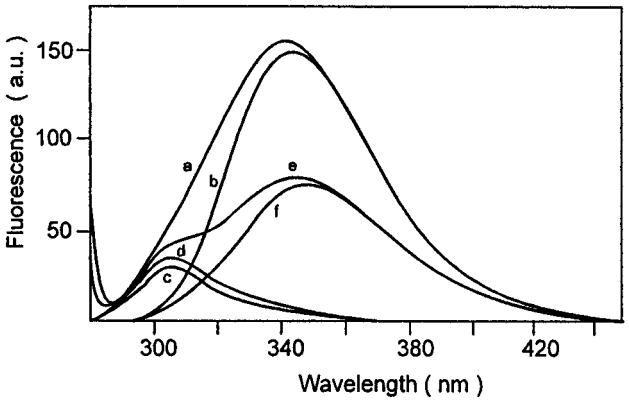

FIGURE 1: Fluorescence spectra of hrIFN-γ in 10 mM Tris-HCl at pH 7.7 excited at 270 nm (a and e) and at 295 nm (b and f). Spectra e and f are obtained after incubation of the protein solution at 50 °C for 90 min. The pairs a and b and e and f are normalized to absorbancy at 380 nm. The difference spectra c (between a and b) and d (between e and f) express the contribution of Tyr residues. Emission spectra a−c characterize predominantly the dimeric forms and d−f the monomeric forms.

excited at 295 nm with that of the standard N-Ac-Trp-NH_2 normalized for the absorbancy at 295 nm. Protein solutions with a concentration higher than 5 μM were used for this experiment. Measurements were performed immediately after dilution of stock protein solutions (15−30 μM) at 20 °C. A value of 0.13 was used for the quantum yield of the standard (Lehrer, 1971). The efficiency of the Tyr to Trp energy transfer was estimated as described by Eisinger (1969).

Time-resolved fluorescence and fluorescence anisotropy decays were measured by using the time-correlated single-photon counting technique (Dorovska-Taran et al., 1994; Pap et al., 1993). The measuring system was able to resolve accurately fluorescence lifetimes of 30 ps. The excitation and the emission wavelengths were 300 and 348 nm, respectively. The experiments were carried out at two temperatures: 20 and 50 °C. The samples incubated for 90 min at 50 °C were measured at this temperature and at 20 °C after cooling. The lifetime and correlation time distributions were determined from the total fluorescence decay and the anisotropy decay by the MEM program (Maximal Entropy Data Consultants Ltd., Cambridge, U.K.). Details are given by Livesey and Brochon (1987).

Native polyacrylamide gel electrophoresis in a homogeneous medium was performed with the Pharmacia Fast System at 15 °C and with a 40 min running time. Fast Gel Media (Homogeneous 20) with stacking gel zones T 7.5%, C 3% and separating gel zones T 20.0%, C 2% were used. The buffer system in the gel was 0.112 M sodium acetate and 0.112 M Tris-HCl at pH 6.5. Fast gel native buffer was 0.88 M L-alanine and 0.25 Tris-HCl at pH 8.8. Protein samples with a concentration of about 1 μM were analyzed. The protein bands were visualised by silver staining.

RESULTS

Fluorescence Properties of Human Recombinant Interferon γ. Fluorescence emission spectra of predominantly dimeric hrIFN-γ are shown in Figure 1 (curves a−c). When excited either at 270 nm (where both Tyr and Trp residues absorb) or at 295 nm (where predominantly Trp absorbs), the spectra are dominated by Trp emission (Figure 1, curves a and b, respectively). The position of the spectral maximum is at 343 nm, and a relative Trp emission quantum yield of 0.042 was calculated. By differential computation of the emission spectra excited at 270 and 295 nm, a weak contribution of Tyr residues (less than 10% of the overall protein fluorescence) could be detected (Figure 1, curve c).

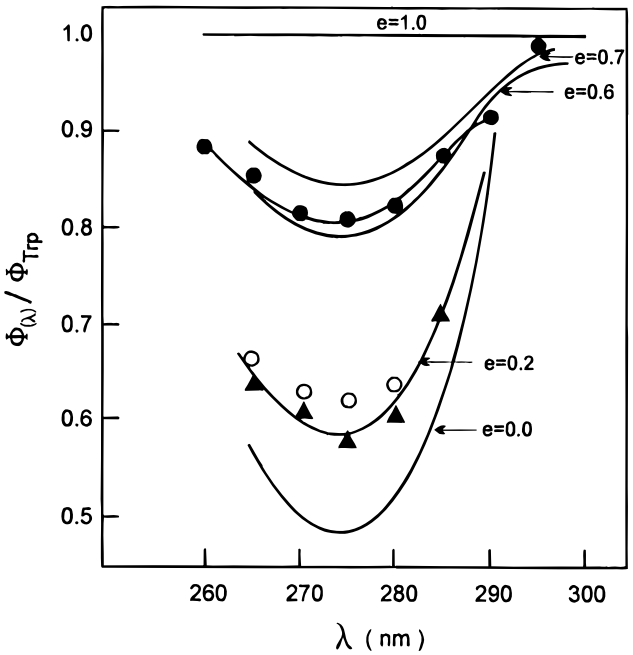

FIGURE 2: Wavelength dependence of the relative quantum yield $\Phi(\lambda)/\Phi_{Trp}$ of 1 μM hrIFN-γ (10 mM Tris-HCl at pH 7.7) measured after incubation of the protein for 90 min at 4 °C (●), at 30 °C (○), and at 47 °C (▲). The solid lines are theoretical curves obtained according to Eisinger (1969) for different values of the energy transfer efficiency e. All theoretical and experimental data are normalized to absorbancy at 295 nm.

The efficiency of the radiationless energy transfer from Tyr to Trp was calculated from the corresponding fluorescence excitation spectra. The best fit of the experimental data to the theoretical curves calculated according to Eisinger (1969) was obtained for a 62% efficiency of the transfer (Figure 2). Thus, about 62% of the excitation energy absorbed by the Tyr residues is transferred via dipole−dipole interactions to the Trp chromophore.

Dependence of the Trp Emission on the Concentration of hrIFN-γ. Dilution of the stock interferon solutions led to a significant reduction of the Trp emission, which was not proportional to the decrease of the protein concentration. This effect became pronounced at concentrations lower than 1 μM. The fluorescence measured at different dilutions was normalized to 1 μM IFN-γ and plotted against the protein concentration. As seen in Figure 3, the experimental points best fit a theoretical curve of a dimer−monomer equilibrium derived by our theoretical model (see Appendix) assuming an equilibrium constant of 3.8×10^{-7} M and a 50% lower quantum yield of the monomer as compared to that of the dimer.

The results from PAGE experiments showed that even at 4 °C a band corresponding to the monomer appears in the gel together with that of the dimer (Figure 5A). This confirms the existence of a dimer−monomer equilibrium.

Kinetic and Thermodynamic Parameters of hrIFN-γ Dissociation. Incubation of 1 μM hrIFN-γ at three different temperatures (13, 30, and 47 °C) led to a decrease of the

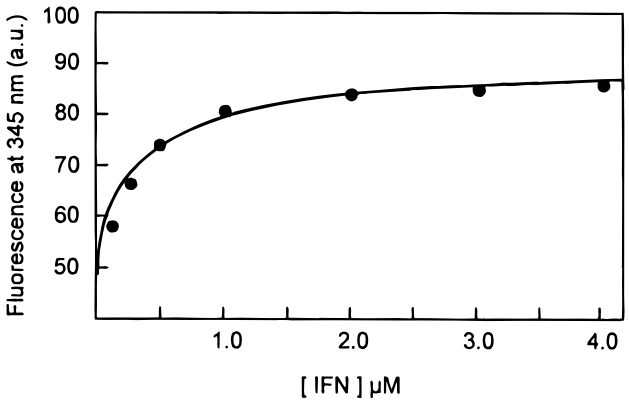

FIGURE 3: Fluorescence maximal intensity at 345 nm, measured after 24 h of incubation of IFN-γ solutions of different concentrations at 13 °C. Excitation was at 295 nm, and the data were normalized to a 1 μM protein concentration. The solid line is a theoretical curve of a monomer−dimer dissociation calculated with an equilibrium constant of 3.8×10^{-7} M^{-1}.

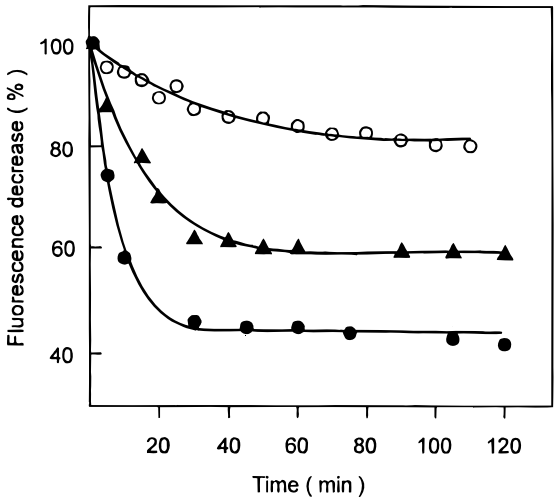

FIGURE 4: Fluorescence intensity decrease at 345 nm of a 1 μM IFN-γ solution incubated at 13 °C (○), at 30 °C (▲), and at 47 °C (●). The solid lines are theoretical curves determined by solving the equations in the Appendix by means of a computer program. They fit well the equilibrium constants in Table 1.

fluorescence intensity. Its value reached a final plateau depending on the temperature (Figure 4). The solid lines describe the dimer−monomer equilibrium of IFN-γ according to the theoretical kinetic model given in the Appendix. They were obtained by selecting the dissociation and association rate constants k_1 and k_{-1} to best fit the experimental data. Their values and that of the equilibrium constants K_e for the corresponding temperatures are given in Table 1. The equilibrium constant at 47 °C is about 2- and 6.6-fold higher than those at 30 and 13 °C, respectively. This was due to the fact that the higher temperature mainly increased dissociation rate constants (Table 1).

The thermodynamic parameters of the dissociation were calculated from the equilibrium constants in Table 1. The latter were derived from the fluorescence decrease taking place during a period of 20−25 min (Figure 4) which is shorter than the time required for a detectable aggregation to start. The free energy change (ΔG) was 8.2 kcal/mol, the enthalpy change (ΔH) 10.1 kcal/mol, and the entropy change (ΔS) on the order of 6 eu. The activation energy (E_{act}) had a value of 12.0 kcal/mol.

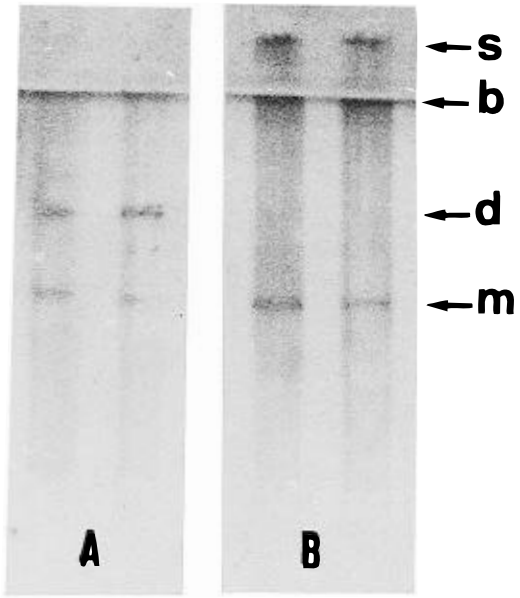

FIGURE 5: Native PAG electrophoresis of 1 μM hrIFN-γ analyzed immediately after preparation (A) or after 60 min of incubation at 47 °C (B): s, start; b, boundary between stacking and separating gels; d, dimers; and m, monomers. Aggregates are seen on the start in part B.

Table 1: Specific Activity and Kinetic Parameters of hrIFN-γ Dissociation at Different Temperatures[a]

T (K)	K_e (M)	k_1 (s^{-1})	k_{-1} (M^{-1} s^{-1})	activity (IU/mg)
286	3.8×10^{-7}	3.8×10^{-4}	1.0×10^{3}	1.7×10^{7}
303	1.4×10^{-6}	1.3×10^{-3}	9.5×10^{2}	−
320	2.5×10^{-6}	3.5×10^{-3}	1.4×10^{3}	0.4×10^{7}

[a] K_e is the equilibrium constant, and k_1 and k_{-1} are the dissociation and association rate constants, respectively, calculated from the fluorescence data (Figure 4) and from the theoretical kinetic model (see Appendix) by a computer program. Standard errors for kinetic and activity measurements were about 5%.

Fluorescence Decay and Fluorescence Anisotropy Decay. The polarized fluorescence decays were measured at 20 and 50 °C and then back at 20 °C. Figure 6 contains a summary of fluorescence and anisotropy decay curves and their MEM reconstructions into lifetime distribution [$\alpha(\tau)$ versus τ] and correlation time distribution [$\beta(\phi)$ versus ϕ]. All relevant parameter values are presented in Table 2. Although the protein monomer contains a single Trp, the fluorescence lifetime distribution consisted of two major components. In the two samples (untreated and incubated at 50 °C), both measured at 20 °C, long-lived components with barycenters at 3.1 and 3.3 ns (after heating) were predominant. At 50 °C, this major lifetime decreased to 2.0 ns and shorter lifetimes of 0.57 and of 0.11 ns appeared (Figure 6 and Table 2).

The fluorescence anisotropy decay at 20 °C was completely dominated by a rotational correlation time with the barycenter at 25 ns (Table 2). It arose from the tumbling of hrIFN-γ dimers and possibly tetramers as suggested by the broadness of the distribution. Incubation of the protein at 50 °C for 90 min caused a dramatic change in the anisotropy decay pattern (Figure 6). The process was characterized by a rapid decay superimposed on a constant anisotropy which was not decaying on the 30 ns experimental time scale. The short correlation time was centred at 3.2 ns. The long decay could not be resolved and was arbitrarily assigned to 100 ns

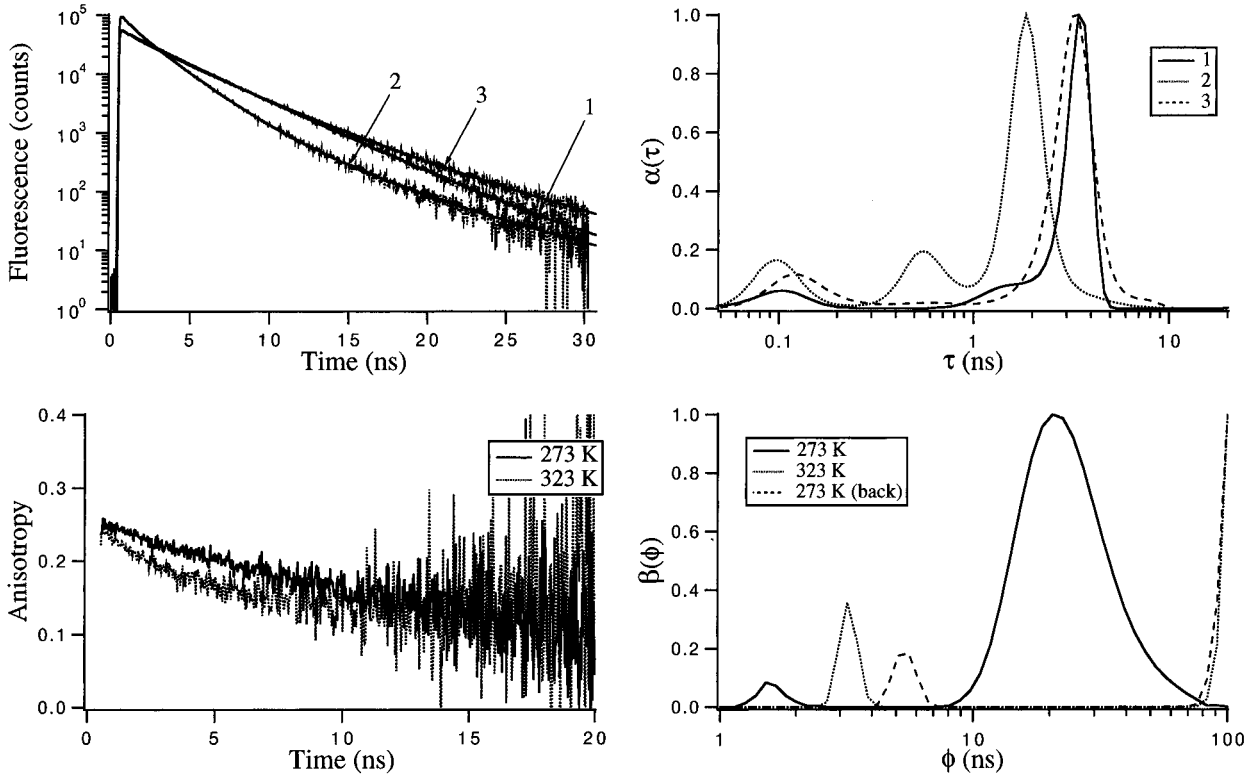

FIGURE 6: (Top) Experimental and fitted fluorescence decays (left) of hrIFN-γ under different conditions: curve 1, at 293 K; curve 2, at 323 K; curve 3, at 293 K after heating at 50 °C for 90 min. The MEM reconstructions are shown on the right. Barycenters (τ) and relative amplitudes (α) are given in Table 2. (Bottom) Experimental anisotropy decay curves constructed from the individual polarized decay curves for hrIFN-γ at 293 and 323 K. The third anisotropy decay curve did not differ from the one at 323 K and is not presented. The MEM reconstructions are shown on the right. Barycenters (ϕ) and relative amplitudes (β) are preseted in Table 2.

Table 2: Fluorescence Lifetimes and Rotational Correlation Times of Tryptophan in hrIFN-γ[a]

T (K)	α_1	τ_1 (ns)	α_2	τ_2 (ns)	α_3	τ_3 (ns)	β_1	ϕ_1 (ns)	β_2	ϕ_2 (ns)	χ^2 [b]
293	0.10	0.11	0.90	3.1	–	–	0.006	1.6	0.246	25	0.99
323	0.15	0.11	0.69	2.0	0.16	0.57	0.096	3.2	0.147	100	1.15
293[c]	0.15	0.15	0.83	3.3	0.02	0.15	0.071	5.4	0.190	100	1.02

[a] Obtained from the main contributions of the MEM of fluorescence decay [$\alpha(\tau)$ versus τ] and fluorescence anisotropy decay analysis [$\beta(\phi)$ versus ϕ]. [b] The reduced χ^2 indicates the quality of the fit. [c] After heating for 90 min at 50 °C.

(Table 2). The short correlation time was probably arising from monomers and confirmed the conclusion that the higher temperature favored the dissociation of the dimers. After the sample was cooled to 20 °C, a correlation time of 5.4 ns was obtained for the monomer. This value is close to the theoretical one for a hydrated, spherical protein of 17 kDa which is the molecular mass of the IFN-γ monomer. The increase from 3.2 to 5.4 ns is in keeping with the dependence of the rotational correlation time on η/T (η = viscosity, T = absolute temperature).

A nonresolved very long correlation time of hrIFN-γ was predominant both in the heated and in the subsequently cooled samples (Figure 6). The appearance of this component strongly suggests the formation of aggregates upon heating which persist after cooling to 20 °C. These data were confirmed by the results from the PAGE performed after incubation of a 1 μM interferon solution at 47 °C for 60 min. Two bands corresponding to protein monomers and aggregates were observed on the gel (Figure 5B).

Biological Activity of hrIFN-γ. hrIFN-γ (1 μM) incubated for 90 min at 13 °C had a specific antiviral activity of 1.7 × 10^7 IU/mg. This activity dropped to 4 × 10^6 IU/mg after incubation of the protein at 47 °C for 90 min; i.e. the heating led to a 4-fold activity reduction (Table 1).

DISCUSSION

The biologically active form of IFN-γ is a homodimer. Each subunit contains one Trp at position 36 and four Tyr residues. The unique Trp is highly conserved in all interferons γ sequenced until now. According to the crystallographic data, it is located at the end of helix B in a burried hydrophobic region formed by Phe 29, Leu 30, Ile 32, and Leu 34 of the same helix (Ealick et al., 1991).

As shown in this study, the fluorescence spectrum of hrIFN-γ is dominated by the emission of the Trp residue with a maximum at 343 nm. This emission position is typical of a chromophore partially exposed to the external medium. A significant part of the Trp fluorescence was found to be due to energy transfer from Tyr residues. Evaluation of the efficiency of this process shows that 62% of the excitation energy absorbed by Tyr residues is transferred via radiationless dipole−dipole interactions to the Trp chromophore (Figure 2). By using the crystallographic coordinates of the C-α atoms (Ealick et al., 1991), distances ranging from 18.5 to 30.1 Å were calculated between the single Trp and the four Tyr residues which theoretically could be involved in the energy transfer within the same domain of the dimer. For the intersubunit energy transfer, the most probable candidate seems to be Tyr 98 (helix E) of the other subunit which is the Tyr residue nearest to Trp 36 (18.5 Å calculated distance). For the intrasubunit interactions, Tyr 53 (helix C) of the same subunit is the chromophore nearest to Trp 36 (calculated distance is 19.2 Å). However, it should be

pointed out that an efficient energy transfer requires not only a short distance but also a proper mutual orientation of the indole and phenol rings.

Sedimentation studies on IFN-γ equilibrium have led to the conclusion that human recombinant IFN-γ is a stable dimer and does not dissociate into monomers at neutral pH (Yphantis & Arakawa, 1987). The crystallographic data have shown that the dimer is stabilized by multiple intersubunit interactions. This has suggested that the separation of the two subunits would be difficult without a significant disruption of their tertiary structure (Ealick et al., 1991).

However, our data show that the dimer exists in a dynamic equilibrium with the monomer. The dimers and the monomers possess different fluorescence properties which allowed detailed studies on the kinetics of the dissociation process. Accumulation of monomers was associated with a significant decrease (about 50%) of the Trp emission (Figure 1, compare curves b and f). However, the position of the emission maximum remained almost constant (343−344 nm), indicating that no dramatic conformational changes in the microenvironment of the single Trp chromophore took place after dissociation of the dimer. This fact should be of critical importance for the reversibility of the association−dissociation process.

Dissociation of the dimer into monomers abolishes the energy transfer between the Trp chromophore and Tyr residues belonging to different subunits of the dimer. While the efficiency of the energy transfer in the dimer was 62%, the efficiency of the same process in the monomer was reduced to 20−25%. This residual efficiency was due to some intrasubunit energy transfer (Figure 2). As expected, this was accompanied by an enhancement of the fractional contribution of the Tyr residues to the overall emission (from about 10% in the dimer to about 30% in the monomer, Figure 1).

The fluorescence decay of the single Trp in hrIFN-γ is heterogeneous. The heterogeneity increases when the protein is heated and subsequently cooled. If it is assumed that dimers and tetramers have a comparable fluorescence lifetime pattern, then this finding is in agreement with the concept that the other forms, monomers and aggregates, have significantly different lifetimes. These results show that the 50% decrease in the Trp emission upon dissociation of the dimer is due not only to a reduction of the Tyr to Trp energy transfer but also to changes in the fluorescence lifetime distribution of excited monomeric species with somewhat shorter lifetimes.

The value calculated for the free energy changes of the dimer dissociation is positive (8.2 kcal/mol). This means that the dimer is the energetically favored species. The dissociation reaction is endothermic (enthalpy changes of 10.1 kcal/mol) and is mainly driven by the entropy changes of the system (an increase of about 6 eu). The relatively high value of the activation energy of the dissociation process (E_{act} = 12.0 kcal/mol) is in agreement with the fact that it is favored by the dilution of the protein solution and by an increase of the temperature. The association rate constants were practically not affected by the temperature within the temperature range studied.

Assuming a value of 0.735 cm^3/g for the partial specific volume and of 0.2 cm^3/g for the degree of hydration at 20 °C (Vos et al., 1987), a correlation time of 13 ns could be theoretically predicted for a rigid sphere with a 35 kDa molecular mass, corresponding to that of an IFN-γ dimer. From MEM analysis of the anisotropy decay at 20 °C, a broad distribution was recovered with the barycenter at 25 ns (Table 2). This is about 2 times higher than the predicted correlation time for the dimer. Even if hrIFN-γ were not a sphere but a flattened ellipsoid with dimensions of about 60 × 40 × 30 Å as suggested by the crystallographic model (Ealick et al., 1991) and if a somewhat higher degree of hydration were assumed, the 25 ns correlation time could not be reconciled with only dimeric species. Given the broadness of the correlation time distribution, it is more probable that a mixture of dimers and tetramers prevails, similarly as found previously for interferon α_2 (Vincent et al., 1992). Dissociation of dimers into monomers and the presence of aggregates is seen when hrIFN-γ is heated at 50 °C for 90 min. This process seems to be irreversible; no correlation time characteristic of dimeric species was found, and no band of the dimer in PAGE was observed after cooling (Figure 5B). In fact, aggregation caused a significant reduction (about 75%) of the antiviral activity of IFN-γ.

In agreement with the data of others (Mulkerrin & Wetzel, 1989), our observations also show that aggregation is a relatively slow process requiring a population of certain monomeric forms competent for aggregation. Thus, during the first 20 min, it does not interfere with the dimer−monomer equilibrium. This explains the very good fitting of the experimental data to a simple monomer−dimer equilibrium model.

Incubation of the protein for 90 min at 50 °C does not seem to thermally denature the sample for the following reasons: (1) a significant antiviral activity is still preserved and (2) the fluorescence parameters of the heated protein are characteristic of a native state. It should be noted that the emission intensity of the thermally denatured protein is reduced by about 30% and the position of its emission maximum is blue-shifted by 11 nm (spectra not shown). Studies on IFN-γ aggregation by other authors (Mulkerrin & Wetzel, 1989) have also shown that thermal denaturation of this protein occurs above 50 °C.

Our data suggest a central role of the dynamic conformational distribution of the monomers for the aggregation process, and we propose the following model for the IFN-γ equilibrium:

$$D \Longleftrightarrow M_1 \Longleftrightarrow \cdots \Longleftrightarrow M_i \Longleftrightarrow \cdots \Longleftrightarrow M_n$$
$$\Downarrow\Uparrow$$
$$A$$

where D is the dimer, M_i represents monomers in different conformational states (conformers), and A represents aggregates. Probably, some monomeric conformers which are more populated at higher temperatures are competent for aggregation. The aggregation of the monomers could be explained by the effect of heating on the α helical structures which before full denaturation may expose hydrophobic surfaces, leading to irregular aggregation.

Human IFN-γ possesses a very high specific activity, and its biological effect *in vivo* shows a concentration optimum (Kleinerman et al., 1986). Thus, the physiological meaning of the monomer−dimer equilibrium (with an inactive monomer) is probably the role of preventing unwanted effects of too high local concentrations before the interferon molecules reach the target cells. In the latter case, the

formation of a dimer−receptor complex can allow the selection of dimers even if the interferon concentration is very low, due to the high-affinity constant of this complex. Aggregates probably do not play an important role for the system *in vivo* being unfavored at physiological temperature and concentrations.

ACKNOWLEDGMENT

The authors are very grateful to Dr. R. Mironova for providing highly purified hrIFN-γ. We thank D. Givkova, A. Vanthoch, and E. Dainese for technical assistance and Prof. M. Beltramini and Dr. F. Ricchelli for their interest.

APPENDIX

The dynamic equilibrium of the dissociation of the dimer A_2 to monomers A

$$A_2 \underset{k_1}{\overset{k_{-1}}{\rightleftharpoons}} 2A$$

according to the law of mass action is described by the following equations:

$$k_1 A_2 = k_{-1} A^2 \tag{1}$$

$$K_e = k_1/k_{-1} \tag{2}$$

$$A_T = 2A_2 + A \tag{3}$$

where A_T is the total protein concentration as monomers and K_e is the equilibrium constant.

The changes of the dimer and of the monomer concentrations could be followed by the differential equations expressing the corresponding reaction rates:

$$dA_2/dt = -k_1 A_2 + k_{-1} A^2 \tag{4}$$

$$dA/dt = k_1 A_2 - k_{-1} A^2 \tag{5}$$

Substituting A_2 and A in eqs 4 and 5 from eq 3, we obtain:

$$dA_2/dt = 4k_{-1}{A_2}^2 - (k_1 + 4k_{-1}A_T)A_2 + k_{-1}{A_T}^2 \tag{6}$$

$$dA/dt = -k_{-1}A^2 - k'_1 A + k'_1 A_T \tag{7}$$

where $k'_1 = k_1/2$.

Taking into account that $(k'_1)^2 \ll 4k_{-1}k'_1 A_T$ and that K_e is on the order of 10^{-8}, as indicated by sedimentation experiments (Yphantis & Arakawa, 1987), the integration of eq 7 from 0 to A gives the following expression for the kinetics of monomer formation:

$$A = \sqrt{\frac{K_e}{2}A_T}\,\frac{1 - e^{-2t\sqrt{-q'}}}{1 + e^{-2t\sqrt{-q'}}} \tag{8}$$

where $q' = -k_{-1}k_1 A_T$.

Equation 8 allows us to calculate the concentration A of the monomer as a function of time. The parameters K_e and q' have been computed by fitting the theoretical function (eq 8) to experimental data (Figure 4). A is related to the registered fluorescence F as follows:

$$F = 2A_2\phi_2 + A\phi_1 \tag{9}$$

or, if we introduce the total concentration A_T, eq 9 becomes:

$$F = A_T\phi_2 - A(\phi_2 - \phi_1) \tag{10}$$

where ϕ_2 and ϕ_1 are the quantum yields of the dimer and of the monomer, respectively.

REFERENCES

Anderson, P., Yip, Y. K., & Vileek, J. (1982) *J. Biol. Chem. 257*, 11301−11304.
Beaven, G. H., & Holiday, E. R. (1952) *Adv. Protein Chem. 7*, 319−325.
Dorovska-Taran, V., van Hoek, A., Link, T. A., Visser, A. J. W. G., & Hagen, W. R. (1994) *FEBS Lett. 348*, 305−310.
Ealick, S. E., Cooc, W. J., Vijay-Kumar, S., Carson, M., Nagabhushan, T. L., Trotta, P. P., & Bugg, C. E. (1991) *Science 252*, 698−702.
Eisinger, G. (1969) *Biochemistry 8*, 3902−3907.
Hsu, Y.-R., & Arakawa, T. (1985) *Biochemistry 24*, 7959−7963.
Kleinerman, E. S., Kurrock, R., Wyatt, D., Quwesada, R., Gutterman, U., & Fidler, I. J. (1986) *Cancer Res. 46*, 5401−5405.
Lehrer, S. S. (1971) *Biochemistry 10*, 3254−3263.
Livesey, A. K., & Brochon, J. C. (1987) *Biophys. J. 52*, 693−706.
Lowry, O. H., Rosebrough, N. L., Farr, A. I., & Randall, B. J. (1951) *J. Biol. Chem. 193*, 265−275.
Mulkerrin, M. G., & Wetzel, R. (1989) *Biochemistry 28*, 6556−6561.
Pap, E. H. W., Bastiaens, P. I. H., Borst, J. W., van den Berg, P. A. W., van Hoek, A., Snoek, G. T., Wirtz, K. W. A., & Visser, A. J. W. G. (1993) *Biochemistry 32*, 13310−13317.
Pestka, S., Langer, J. A., Zoon, K. C., & Sammel, C. E. (1987) *Annu. Rev. Biochem. 56*, 727−777.
Rubinstein, S., Familletti, P. C., & Pestka, S. (1981) *J. Virol. 37*, 755−759.
Vincent, M., Li De La Sierra, I. M., Berberan-Santos, M. N., Diaz, A., Diaz, M., Padron, G., & Gallay, J. (1992) *Eur. J. Biochem. 210*, 953−961.
Vos, K., van Hoek, A., & Visser, A. J. W. G. (1987) *Eur. J. Biochem. 165*, 55−63.
Yphantis, D. A., & Arakawa, T. (1987) *Biochemistry 26*, 5422−5427.

BI9527597